

HELIUM NOVA ON A VERY MASSIVE WHITE DWARF – A LIGHT CURVE MODEL OF V445 PUPPIS (2000) REVISED

MARIKO KATO

Department of Astronomy, Keio University, Hiyoshi, Kouhoku-ku, Yokohama 223-8521, Japan

IZUMI HACHISU

Department of Earth Science and Astronomy, College of Arts and Sciences, University of Tokyo, Komaba, Meguro-ku, Tokyo 153-8902, Japan

SEIICHIRO KIYOTA

4-405-1003 Matsushiro, Tsukuba 305-0035, Japan

AND

HIDEYUKI SAIO

Astronomical Institute, Graduate School of Science, Tohoku University, Sendai 980-8578, Japan

to appear in the Astrophysical Journal

ABSTRACT

V445 Pup (2000) is a unique object identified as a helium nova. Color indexes during the outburst are consistent with those of free-free emission. We present a free-free emission dominated light curve model of V445 Pup on the basis of the optically thick wind theory. Our light curve fitting shows that (1) the white dwarf (WD) mass is very massive ($M_{\text{WD}} \gtrsim 1.35 M_{\odot}$), and (2) a half of the accreted matter remains on the WD, both of which suggest that the increasing WD mass. Therefore, V445 Pup is a strong candidate of Type Ia supernova progenitor. The estimated distance to V445 Pup is now consistent with the recent observational suggestions, $3.5 \lesssim d \lesssim 6.5$ kpc. A helium star companion is consistent with the brightness of $m_v = 14.5$ mag just before the outburst, if it is a little bit evolved hot ($\log T$ (K) $\gtrsim 4.5$) star with the mass of $M_{\text{He}} \gtrsim 0.8 M_{\odot}$. We then emphasize importance of observations in the near future quiescent phase after the thick circumstellar dust dissipates away, especially its color and magnitude to specify the nature of the companion star. We have also calculated helium ignition masses for helium shell flashes against various helium accretion rates and discussed the recurrence period of helium novae.

Subject headings: binaries: close — novae, cataclysmic variables — stars: individual (V445 Pup) — stars: mass loss — white dwarfs

1. INTRODUCTION

The outburst of V445 Pup was discovered on 30 December 2000 by Kanatsu (Kato & Kanatsu 2000). The outburst shows unique properties such as absence of hydrogen, unusually strong carbon emission lines as well as strong emission lines of Na, Fe, Ti, Cr, Si, Mg etc. (Ashok & Banerjee 2003; Iijima & Nakanishi 2007). The spectral features resemble those of classical slow novae except absence of hydrogen and strong emission lines of carbon (Iijima & Nakanishi 2007). The development of the light curve is very slow (3.3 mag decline in 7.7 months) with a small outburst amplitude of 6 mag. From these features, this object has been suggested to be the first example of helium novae (Ashok & Banerjee 2003; Kato & Hachisu 2003).

In our earlier work (Kato & Hachisu 2003) we presented a theoretical light curve model with the assumption of black-body emission from the photosphere, which resulted in the best fit model of a very massive white dwarf (WD) ($M_{\text{WD}} \gtrsim 1.3 M_{\odot}$) and a relatively short distance of $d \lesssim 1$ kpc. However, Iijima & Nakanishi (2007) recently showed that there are absorption lines of Na I D1/2 at the velocities of 16.0 and 73.5 km s⁻¹, suggesting that V445 Pup is located in or beyond the Orion arm and its distance is as large as 3.5–6.5

kpc. Woudt & Steeghs (2008) also suggested a large distance of 4.9 kpc. Moreover, color indexes during the outburst are consistent with those of free-free emission. With these new observational aspects we have revised the light curve model of V445 Pup.

Helium novae were theoretically predicted by Kato et al. (1989) as a nova outburst caused by a helium shell flash on a white dwarf. Such helium novae have long been a theoretical object until the first helium nova V445 Pup was discovered in 2000. Kato et al. (1989) assumed two types of helium accretion: one is helium accretion from a helium star companion, and the other is hydrogen-rich matter accretion with a high accretion rate and, beneath the steady hydrogen burning shell, ash helium accumulates on the WD. The latter case is divided into two kinds of systems depending on whether hydrogen shell burning is steady (stable) or not. To summarize, helium accretion onto a WD occurs in three types of systems: (1) helium accretion from a helium star companion; (2) steady hydrogen accretion with a rate high enough to keep steady hydrogen shell burning such as supersoft X-ray sources, e.g., RX J0513.9-6951 (e.g., Hachisu & Kato 2003; McGowan et al. 2006) and CAL 83 (e.g., Schmidtke & Cowley 2006), (3) hydrogen accretion with a relatively low rate resulting in a recurrent nova such as RS Oph (e.g., Hachisu et al. 2007) and U Sco (e.g., Hachisu et al. 2000). In the present paper, we regard that V445 Pup is Case (1), because no hydrogen lines were detected (Iijima & Nakanishi 2007).

Electronic address: mariko@educ.cc.keio.ac.jp
Electronic address: hachisu@ea.c.u-tokyo.ac.jp
Electronic address: skiyota@nias.affrc.go.jp
Electronic address: saio@astr.tohoku.ac.jp

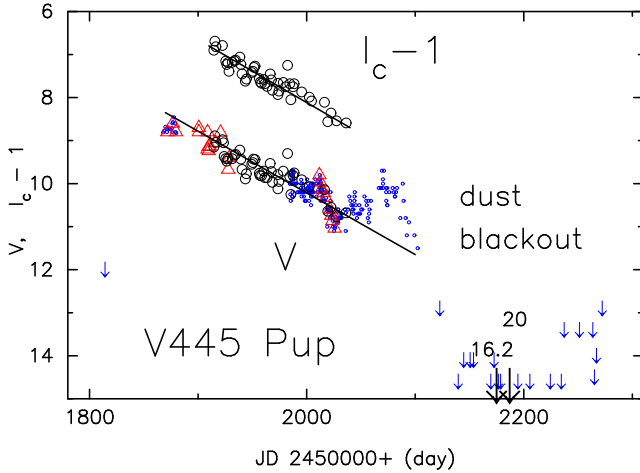


FIG. 1.— V and I_c light curves of V445 Pup (large open circles). The I_c data are shifted up by one magnitude in order to separate it from the V light curve. Open triangles denote V magnitudes (IAUC No. 7552, 7553, 7557, 7559, 7569, 7620). Small open circles and downward arrows are taken from AAVSO to show very early and later phases of the outburst. Large downward arrows show an upper limit observation of $I_c > 16.2$ (this work), $V > 20$ and $I > 19.5$ (Henden et al. 2001). Straight lines indicate the average decline rates of $1.9 \text{ mag}/130 \text{ days} = 0.0146 \text{ mag day}^{-1}$ and $3.3 \text{ mag}/230 \text{ days} = 0.0143 \text{ mag day}^{-1}$ for I_c and V , respectively.

In helium novae, mass loss owing to optically thick wind is relatively weak compared to hydrogen novae, and a large part of the accreted helium burns into carbon and oxygen and accumulates on the WD (Kato & Hachisu 1999, 2004). Our previous model indicated that V445 Pup contains a massive WD ($M_{\text{WD}} \gtrsim 1.3 M_{\odot}$) and the WD mass is increasing through helium shell flashes. Therefore, V445 Pup is a strong candidate of Type Ia supernova progenitors. Although there are two known evolutionary paths of the single degenerate scenario toward Type Ia supernova (e.g., Hachisu, Kato & Nomoto 1999), helium accreting WDs such as V445 Pup do not belong to either of them. Therefore, it may indicate the third path to Type Ia supernovae. If various binary parameters of V445 Pup are determined, they provide us important clues to binary evolutions to Type Ia supernovae.

In the next section we introduce our multi-band photometric observations, which indicates that free-free emission dominates in optical and near infrared. In §3 we present our free-free emission dominated light curve model and its application to V445 Pup. Then we discuss brightness in quiescence in §4. Discussion and conclusions follow in §5 and §6, respectively.

2. OBSERVATION

Shortly after the discovery of V445 Pup outburst, one of us (S.K.) started multi-band photometry with a 25.4 cm telescope [focal length = 1600 mm, CCD camera = Apogee AP-7 (SITE SIA502AB of 512×512 pixels)]. V and R_c magnitudes are obtained from January 4 to May 6, 2001, and I_c from January 4, 2001 to January 15, 2007, with the comparison star, TYC 6543-2917-1 ($V = 8.74$, $B - V = 0.304$). All of our data can be taken from the data archive of Variable Star Observers League in Japan (VSOLJ)¹.

Figure 1 shows our V and I_c magnitudes as well as other observations taken from literature. These two light curves show very slow evolution ($\sim 0.014 \text{ mag day}^{-1}$) followed by an oscillatory behavior in the V magnitude before it quickly darkened by dust blackout on about JD 2452100, i.e.,

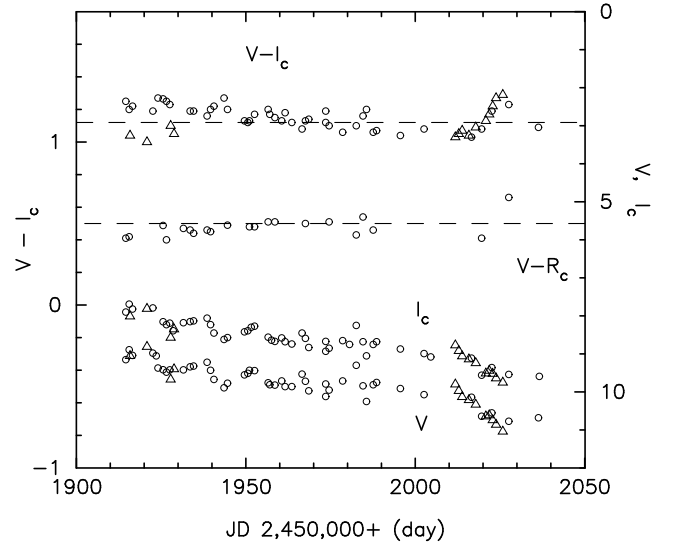


FIG. 2.— Color indexes of $V - I_c$ and $V - R_c$ as well as I_c and V . Open circles: this work. Open triangles: Gilmore (IAUC 7559, 7569) and Gilmore & Kilmartin (IAUC 7620). The horizontal dashed lines indicate the mean values of $V - R_c = 0.5$ and $V - I_c = 1.12$.

7.5 months after the discovery (Henden et al. 2001; Woudt 2002; Ashok & Banerjee 2003). Here, we assume the decline rate of the light curves as shown in Figure 1 ignoring the later oscillatory phase (JD 2452040 – 2452100) because we assume steady-state in the nova envelope as mentioned below and, as a result, our theoretical light curve cannot treat unsteady oscillations.

Figure 2 shows evolution of color indexes $V - I_c$ and $V - R_c$ as well as V and I_c themselves. We can see that both of $V - I_c$ and $V - R_c$ are almost constant with time, i.e., ≈ 1.12 and ≈ 0.5 , respectively, during our observation. This means that the three light curves of V , I_c , and R_c are almost parallel and each light curve shape is independent of wavelength. These are the characteristic properties of free-free emission dominated light curves as explained below.

The flux of optically thin free-free emission is inversely proportional to the square of wavelength, i.e., $F_{\lambda} \propto \lambda^{-2}$. This spectrum shape is unchanged with time although the electron temperature rises during nova outburst because the emission coefficient depends only very slightly on the electron temperature (e.g., Brown and Mathews 1970). Therefore, the color indexes of free-free emission dominated light curves are unchanged with time. On the other hand, the color indexes change with time if blackbody emission dominates because the photospheric temperature rises with time in nova outbursts. Figures 1 and 2 indicate that the emission from V445 Pup is dominated by free-free emission rather than by blackbody emission.

The color index of free-free emission is calculated from $\lambda F_{\lambda} \propto \lambda^{-1}$. When the reddening is known, the reddened color is obtained as

$$m_V - m_{\lambda} = (M_V - M_{\lambda})_0 + c_{\lambda} E(B - V), \quad (1)$$

where $(M_V - M_{\lambda})_0$ is the intrinsic color and c_{λ} is the reddening coefficient (these values are tabulated in Table 4 in Hachisu et al. (2007) for five colors of $V - R$, $V - I$, $V - J$, $V - H$, and $V - K$). Figure 3 shows the color indexes relative to V for two cases of reddening, i.e., $E(B - V) = 0$ and 0.5 .

For comparison, we have added four relative colors of V1500 Cyg (Hachisu & Kato 2006) because its con-

¹ <http://vsolj.cetus-net.org/>

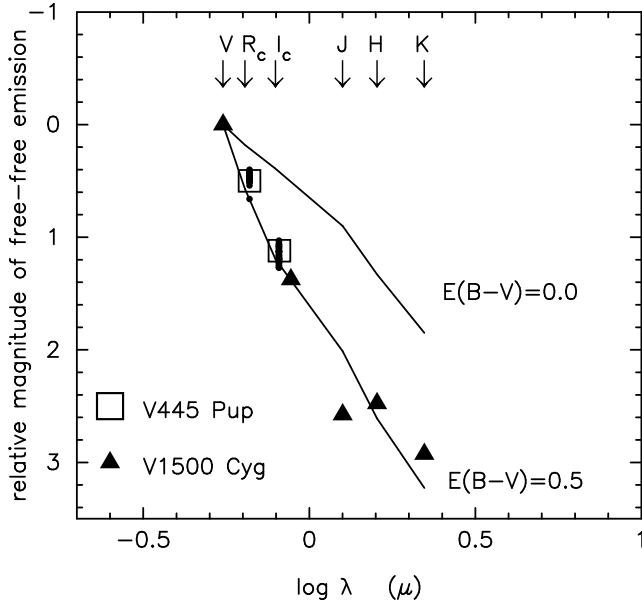


FIG. 3.— Color indexes against wavelength. Our observational color indexes of V445 Pup, $V - R_c$ and $V - I_c$, are plotted for individual data (dots) and their mean values of 0.5 and 1.12 (open squares). The color indexes of V1500 Cyg are added for y magnitude instead of V (filled triangles) (taken from Hachisu et al. 2007). Arrows indicate the effective wavelength of six bands of V , R , I , J , H , and K . Solid curves denote color indexes of free-free emission for $E(B - V) = 0$ and 0.5 .

tinuum flux is known to be that of free-free emission (Gallagher & Ney 1976) except for the first few days after the optical peak. Here we use Strömgren y magnitude instead of V , because the intermediate-wide y band is almost emission-line free. Three ($y - I$, $y - H$, and $y - K$) of four color indexes are consistent with those of color indexes with $E(B - V) = 0.5$ (Ferland 1977; Hachisu & Kato 2006). The J band is strongly contaminated with strong emission lines of He I (e.g. Black & Gallagher 1976; Kolotilov & Liberman 1976; Shenavrin & Moroz 1976). This is the reason why the $y - J$ color index deviates from that of free-free emission (see Hachisu, Kato, & Cassatella 2007, for more details).

Our observed color indexes are shown in Figure 3. The open squares are centered at the mean values of $V - R_c = 0.5$ and $V - I_c = 1.12$, whereas dots represent individual observations. In V445 Pup, no strong emission lines dominate the continuum in V , R , and I bands (Kamath & Anupama 2002; Iijima & Nakanishi 2007). Therefore we conclude that the color indexes of V445 Pup are consistent with those of free-free emission with the reddening of $E(B - V) = 0.51$ (Iijima & Nakanishi 2007).

3. MODELING OF NOVA LIGHT CURVES

3.1. Basic Model

After a thermonuclear runaway sets in on the surface of a WD, the envelope expands to a giant size and the optical luminosity reaches its maximum. Optically thick winds occur and the envelope reaches a steady state. Using the same method and numerical techniques as in Kato & Hachisu (1994, 2003), we have followed evolution of a nova by connecting steady state solutions along the sequence of decreasing envelope mass. We have solved the equations of motion, continuity, radiative diffusion, and conservation of energy, from the bottom of the helium envelope through the photosphere. The winds are accelerated deep inside the photosphere. Updated OPAL opacities are used (Iglesias & Rogers

TABLE 1
MODEL PARAMETERS^a

M_{WD} (M_{\odot})	$\log R_{\text{WD}}$ (R_{\odot})	Y	$X_{\text{C+O}}$
1.2	-2.193	0.68	0.3
1.3	-2.33	0.48	0.5
1.33	-2.417	0.38	0.6
1.35	-2.468	0.38	0.6
1.37	-2.535	0.58	0.4
1.37	-2.535	0.38	0.6
1.37	-2.535	0.18	0.8
1.377	-2.56	0.38	0.6

^a The heavy element content is assumed to be $Z = 0.02$ that includes carbon and oxygen by the solar ratio.

1996). As one of the boundary conditions for our numeral code, we assume that photons are emitted at the photosphere as a blackbody with a photospheric temperature, T_{ph} . Kato & Hachisu (2003) calculated the visual magnitude M_V on the basis of blackbody emission and constructed the light curves. In the present work, we calculate free-free emission dominated light curves. The envelope structure, wind mass loss rate, photospheric temperature, and photospheric radius of the WD envelope are essentially the same as those in the previous model.

The flux of free-free emission from the optically thin region outside the photosphere dominates in the continuum flux of optical and near infrared wavelength region and is approximated by

$$F_{\nu} \propto \int N_e N_i dV \propto \int_{R_{\text{ph}}}^{\infty} \frac{\dot{M}_{\text{wind}}^2}{v_{\text{ph}}^2 r^4} r^2 dr \propto \frac{\dot{M}_{\text{wind}}^2}{v_{\text{ph}}^2 R_{\text{ph}}}, \quad (2)$$

where F_{ν} is the flux at the frequency ν , N_e and N_i are the number densities of electrons and ions, respectively, V is the volume, R_{ph} is the photospheric radius, \dot{M}_{wind} is the wind mass loss rate, and v_{ph} is the photospheric velocity (Hachisu & Kato 2006; Hachisu et al. 2007).

The proportionality constant in equation (2) cannot be determined a priori because we do not calculate radiative transfer outside the photosphere: These proportionality constant are determined by fitting with observational data (Hachisu & Kato 2006; Hachisu and Kato 2007; Hachisu et al. 2007).

3.2. Free-free Light Curve and WD Mass

We have calculated free-free emission dominated light curves of V445 Pup for WD masses of 1.2, 1.3, 1.33, 1.35, 1.37, and 1.377 M_{\odot} . The last one is the upper limit of the mass-accreting WDs (Nomoto et al. 1984). The adopted WD radius and chemical composition are listed in Table 1. Here we assume that chemical composition is constant throughout the envelope.

Figure 4 shows the calculated free-free light curves. More massive WDs show faster decline. This is mainly because the more massive WDs have the less massive envelope and the smaller mass envelope is quickly taken off by the wind. The figure also shows two additional models of $M_{\text{WD}} = 1.37 M_{\odot}$ with different compositions of $X_{\text{C+O}} = 0.4$ and 0.8 . These models show almost similar decline rates to that of $M_{\text{WD}} = 1.37 M_{\odot}$ with $X_{\text{C+O}} = 0.6$.

The starting point of our model light curve depends on the initial envelope mass. When an initial envelope mass is given,

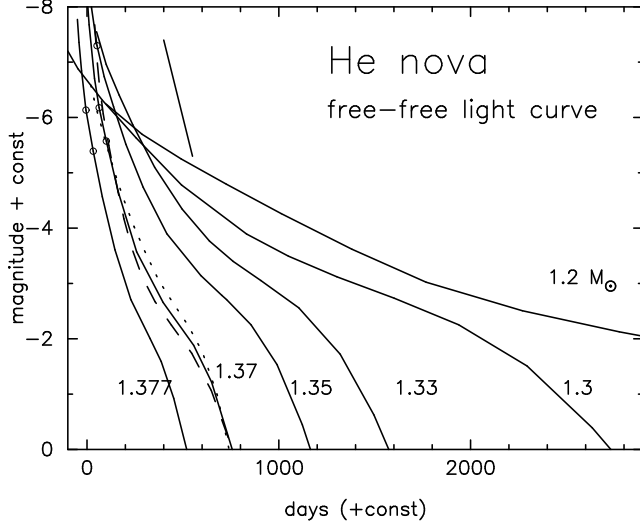


FIG. 4.— Free-free emission dominated light curves for various WD masses. The chemical composition is assumed to be $Y = 0.38$, $X_{C+O} = 0.6$, and $Z = 0.02$ throughout the envelope. The WD mass is attached to each curve. The dashed and dotted curves denote $M_{WD} = 1.37 M_{\odot}$ model but with different chemical composition of $X_{C+O} = 0.4$ and 0.8 , respectively. Small open circles denote the starting points of light curve fitting in Fig. 5: upper and lower points of $M_{WD} = 1.37 M_{\odot}$ (solid line) correspond to Models 4 and 3 and those of $1.377 M_{\odot}$ correspond to Models 8 and 7, respectively. A short solid line indicates the decline rate of observed V data in Fig. 1 (3.3 mag / 230 days).

our nova model is located somewhere on the light curve. For a more massive ignition mass, it starts from an upper point of the light curve. Then the nova moves rightward with the decreasing envelope mass due to wind mass loss and nuclear burning.

The development of helium shell flashes is much slower than that of hydrogen shell flashes mainly because of much larger envelope masses of helium shell flashes (Kato & Hachisu 1994). The short straight solid line in Figure 4 represents the decline rate of V light curve in Figure 1. The length of the line indicates the observed period which is relatively short because of dust blackout 230 days after the optical maximum. We cannot compare the entire evolution period of the light curve with the observational data so that fitting leaves some ambiguity in choosing the best fit model. Even though, we may conclude that WDs with masses of $M_{WD} \lesssim 1.33 M_{\odot}$ are very unlikely because their light curves are too slow to be comparable with the observation.

Figure 5 represents the light curve fitting with observational data. Here, the model light curves of I_c are identical to those of V but are lifted up by 1.12 mag, which is the mean value of $V - I_c$ obtained in Figure 2. It should be noted that, in this figure, these light curves are further lifted up by 1.0 mag because of $I_c - 1$.

These light curves are a part of the model light curves in Figure 4. In the early phase of the outburst the light curve declines almost linearly so that fitting is not unique. We can fit any part of our model light curve if its decline rate is the same as $\approx 0.014 - 0.015 \text{ mag day}^{-1}$, for example, either top or middle part of the same light curve of $1.377 M_{\odot}$ WD in Figure 4. In such a case we show two possible extreme cases, i.e., the earliest starting point and the latest one by open circles, as shown in Figure 4. These model parameters are summarized in Table 2, where we distinguish the model by model number.

Thus we have selected several light curves which show a reasonable agreement with the observation. However, we can-

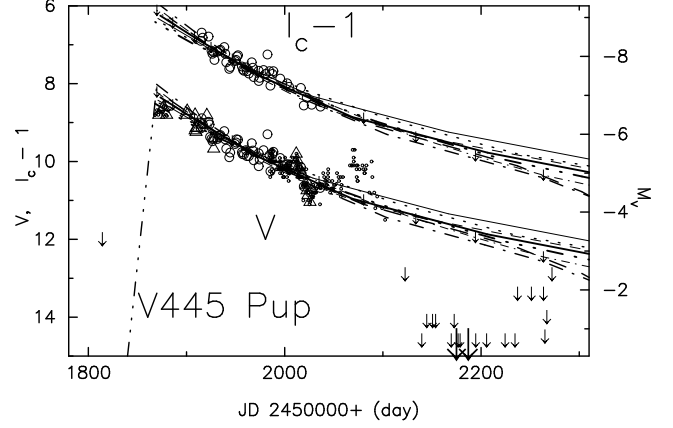


FIG. 5.— Our model light curves are fitted with the observation. Dotted line: Model 1. Thin dashed line: Model 2. Thin solid line: Model 3. Thick solid line: Model 4. Dash-three dotted line: Model 5. Thin dash-dotted line: Model 6. Dashed line: Model 7. Dash-dotted line: Model 8. Our model I_c light curves are identical with those of V but are lifted up by 1.12 mag (and further shifted up by 1 mag for $I_c - 1$). The ordinate on the right vertical axis represents the absolute magnitude of Model 4. For the other models, the model light curves are shifted down by 0.4 mag (Model 1), up by 0.2 mag (Model 2) up by 0.3 mag (Models 3 and 7), down by 0.2 mag (Model 5), down by 0.5 mag (Model 6), up by 0.1 mag (Model 8). The observational data are same as those in Fig. 1.

not choose the best fit model among them because the observed period is too short to discriminate a particular light curve from others because the difference among them appears only in a late stage.

For relatively less massive WDs of $M_{WD} \lesssim 1.33 M_{\odot}$, we cannot have reasonable fits with the observation for any part of the model light curves. Among relatively more massive WDs of $M_{WD} \gtrsim 1.35 M_{\odot}$ in Table 2, Model 1 shows slightly slower decline. Therefore, the $1.35 M_{\odot}$ WD may be the lowest end for the WD mass. Thus we may conclude that V445 Pup contains a very massive WD of $M_{WD} \gtrsim 1.35 M_{\odot}$.

3.3. Mass Accumulation Efficiency

During helium nova outbursts, a part of the helium envelope is blown off in winds, while the rest accumulates on the WD. We define the mass accumulation efficiency, η_{He} , as the ratio of the envelope mass that remains on the WD after the helium nova outburst to the helium envelope mass at ignition, $\Delta M_{He,ig}$ (Kato & Hachisu 2004).

The mass accumulation efficiency is estimated as follows. We have calculated the mass lost by winds during the outburst, ΔM_{ej} . Note that ΔM_{ej} is the calculated total ejecta mass which is ejected during the wind phase, and not the mass ejected during the observing period which may be shorter than the wind phase.

The ignition mass is approximated by the envelope mass at the optical peak, i.e., $\Delta M_{He,ig} \approx \Delta M_{He,peak}$. Since the exact time of the optical peak is unknown, we assume that the optical peak is reached on JD 2451872, i.e., the earliest pre-discovery observation in the brightest stage reported to IAU Circular No. 7553, 28 days earlier than the discovery. The envelope mass at the optical peak is estimated from our wind solution and is listed as $\Delta M_{He,ig}$ in Table 2. The resultant accumulation efficiency,

$$\eta_{He} \equiv \frac{\Delta M_{He,peak} - \Delta M_{ej}}{\Delta M_{He,peak}}, \quad (3)$$

is also listed in Table 2. The efficiencies are as high as $\sim 50\%$. The WD of V445 Pup is already very massive

TABLE 2
PARAMETERS OF FITTED MODEL

model No.	M_{WD} (M_{\odot})	Y	$X_{\text{C+O}}$	$\Delta M_{\text{He,ig}}^{\text{a}}$ (M_{\odot})	$\Delta M_{\text{ej}}^{\text{b}}$ (M_{\odot})	$\eta_{\text{He}}^{\text{c}}$	Distance (kpc)	$\dot{M}_{\text{He}}^{\text{d}}$ ($M_{\odot} \text{ yr}^{-1}$)	$\tau_{\text{rec}}^{\text{d}}$ (yr)
1	1.35	0.38	0.6	3.3E-4	1.8E-4	0.45	6.6	6.E-8	5000
2	1.37	0.58	0.4	1.6E-4	9.2E-5	0.42	5.0	7.E-8	2000
3	1.37	0.38	0.6	1.9E-4	8.7E-5	0.53	4.8	6.E-8	3000
4	1.37	0.38	0.6	2.1E-4	1.1E-4	0.49	5.5	5.E-8	4000
5	1.37	0.18	0.8	3.5E-4	1.2E-4	0.64	6.0	4.E-8	9000
6	1.37	0.18	0.8	3.8E-4	1.5E-4	0.61	6.9	4.E-8	10000
7	1.377	0.38	0.6	1.8E-4	7.4E-5	0.60	4.8	5.E-8	4000
8	1.377	0.38	0.6	2.2E-4	9.6E-5	0.56	5.2	4.E-8	5000

^a Envelope mass at ignition is assumed to be equal to the mass at the optical peak, which we assume as JD 2451872 (28 days before the discovery).

^b Total mass ejected by the wind

^c Mass accumulation efficiency

^d estimated from Fig. 7

($M_{\text{WD}} \gtrsim 1.35 M_{\odot}$) and its mass has increased through helium nova outbursts. Therefore, V445 Pup is a strong candidate of Type Ia supernova progenitors.

4. QUIESCENT PHASE

Before the 2000 outburst, there was a 14.5 mag star at the position of V445 Pup (taken from the archive of VSNET²), but no bright star has been observed since the dust blackout. We may regard that 14.5 mag is the preoutburst magnitude of the binary. There are two possible explanations for this quiescent phase luminosity, one is the accretion disk luminosity and the other is the luminosity of bright companion star. In the following subsections, we discuss how these possible sources contribute to the quiescent luminosity.

4.1. Accretion Disk

In some nova systems, an accretion disk mainly contributes to the brightness in their quiescent phase. If the preoutburst luminosity of V445 Pup comes from an accretion disk, its absolute magnitude is approximated by

$$M_V(\text{obs}) = -9.48 - \frac{5}{3} \log \left(\frac{M_{\text{WD}}}{M_{\odot}} \frac{\dot{M}_{\text{acc}}}{M_{\odot} \text{ yr}^{-1}} \right) - \frac{5}{2} \log(2 \cos i), \quad (4)$$

where M_{WD} is the WD mass, \dot{M}_{acc} the mass accretion rate, and i the inclination angle (equation (A6) in Webbink et al. 1987). Assuming that $M_{\text{WD}} = 1.37 M_{\odot}$ and $i = 80^\circ$ (Woudt & Steeghs 2008), we have $M_V = 1.4, 2.3$, and 3.1 for the accretion rates of $1 \times 10^{-6}, 3 \times 10^{-7}$, and $1 \times 10^{-7} M_{\odot} \text{ yr}^{-1}$, respectively.

The apparent magnitude of the disk is calculated from

$$m_V - M_V = A_V + 5 \log D_{10}, \quad (5)$$

where D_{10} is the distance divided by 10 pc. With the absorption of $A_V = 1.6$ and the distance of 3 kpc, the apparent magnitude is estimated to be $m_V = 15.4, 16.3$ and 17.1 , for the above accretion rates, respectively. For the distance of 6.5 kpc, we obtain brightnesses of $m_V = 17.1, 18.0$, and 18.8 , respectively. All of these values are much fainter than 14.5 mag. Therefore, it is very unlikely that an accretion disk mainly contributes to the preoutburst luminosity.

² <http://vsnet.kusastro.kyoto-u.ac.jp/vsnet/>

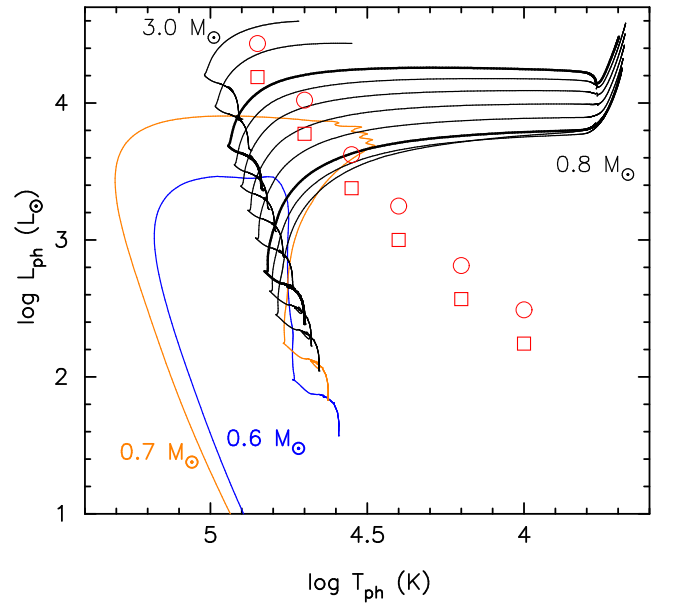


FIG. 6.— Evolutional tracks of helium stars with masses of $M_{\text{He}} = 0.6, 0.7, 0.8, 0.9, 1.0$ (thick line), $1.2, 1.4, 1.6, 1.8, 2.0$ (thick line), 2.5 , and $3.0 M_{\odot}$ in the H-R diagram. The 0.6 and $0.7 M_{\odot}$ stars evolve blueward and do not become red giants. We stopped calculation when carbon ignites at the center for 2.5 and $3.0 M_{\odot}$ stars. Open circles and squares denote stars with a 14.5 mag brightness at the distance of 6.5 kpc and 4.9 kpc, respectively, for $A_V = 1.6$.

4.2. Helium Star Companion

Another possible source of the preoutburst brightness is a helium star companion. Figure 6 shows evolutional tracks of helium stars with masses between 0.6 and $3.0 M_{\odot}$ from the helium main-sequence to the red giant stage in the H-R diagram. We use OPAL opacities and an initial chemical composition of $X = 0.0, Y = 0.98$ and $Z = 0.02$. The numerical method and input physics are the same as those in Saio (1995).

As shown in Figure 6, low mass helium stars do not evolve to a red giant. In our new calculation, the $0.8 M_{\odot}$ helium star evolves to a red giant, but the 0.6 and $0.7 M_{\odot}$ helium stars evolve toward blueward. Paczyński (1971) showed that stars of $M_{\text{He}} \gtrsim 1.0 M_{\odot}$ evolve to a red giant while $0.5, 0.7$, and $0.85 M_{\odot}$ do not. Our calculations are essentially the same as those of Paczyński (1971) and the difference is attributed mainly to the difference between the adopted opacities.

Figure 6 also shows locations of stars whose apparent mag-

nitudes are $m_V = 14.5$ for $A_V = 1.6$. Here, the distance is assumed to be 4.9 (open squares) or 6.5 kpc (open circles). For example, a star of (temperature, luminosity) = $(\log T_{\text{ph}} \text{ (K)}, \log L_{\text{ph}}/L_{\odot}) = (4.2, 2.81)$, $(4.4, 3.25)$, and $(4.6, 3.75)$ could be observed as a 14.5 mag star for 6.5 kpc and $(\log T_{\text{ph}} \text{ (K)}, \log L_{\text{ph}}/L_{\odot}) = (4.2, 2.57)$, $(4.4, 3.0)$, and $(4.6, 3.51)$ for 4.9 kpc. Therefore, the observed 14.5 mag is consistent with the luminosities and temperatures of slightly evolved helium stars of $M_{\text{He}} \gtrsim 0.8 M_{\odot}$ if the companion is a blue star of $\log T_{\text{ph}} \gtrsim 4.5$.

On the other hand, if the companion is redder than $\log T_{\text{ph}} \lesssim 4.4$, there is no corresponding evolution track in the low luminosity region of the H-R diagram as shown in Figure 6. In such a case the preoutburst luminosity cannot be attributed to a helium star companion. Kato (2001)³ suggested that preoutburst color of V445 Pup was much bluer than that of symbiotic stars (which have a red giant companion) but rather close to that of cataclysmic variables (main-sequence or little bit evolved companion). This argument is consistent with our estimate of relatively high surface temperature $\log T_{\text{ph}} \gtrsim 4.5$ (see Fig. 6).

5. DISCUSSIONS

5.1. Distance

As explained in §§3.1 and 3.2, we do not solve energy transfer outside the photosphere and, thus, we cannot determine the proportionality constant in equation (2). Therefore, we cannot determine the distance to V445 Pup directly from the comparison of theoretical absolute magnitude with the observational apparent magnitude. Instead, we can approximately estimate the distance by assuming that the free-free flux is larger than the blackbody flux during the observing period. This assumption gives a lower limit to the distance. We expect that the distance estimated thus is close to the real value. The 8th column of Table 2 lists the distance estimated for each model. These distances are consistent with the observational estimates of $3.5 \lesssim d \lesssim 6.5$ kpc (Iijima & Nakanishi 2007) and ~ 4.9 kpc (Woudt & Steeghs 2008).

5.2. Helium Ignition Mass and Recurrence Period

We have calculated evolution of C+O white dwarfs accreting helium at various rates until the ignition of a helium shell flash. Chemical compositions assumed are $X_{\text{C}} = 0.48$ and $X_{\text{O}} = 0.50$ for the WD core, and $X = 0.0$ and $Y = 0.98$ for the accreted envelope. The initial model adopted for a given core mass and accretion rate is a steady-state model in which the heating due to the accretion is balanced with the radiative energy flow. Adopting such an initial model is justified because the WD has accreted matter from the companion for a long time and experienced many shell flashes.

As the helium accretion proceeds, the temperature at the bottom of the envelope gradually increases. When the temperature becomes high enough the triple-alpha reaction causes a shell flash. The mass of the helium envelope at the ignition depends on the WD mass and the accretion rate as shown in Figure 7. The envelope mass required to ignite a shell flash tends to be smaller for a higher accretion rate and for a larger WD mass. Helium flashes are weaker for higher accretion rates and lower WD masses. In particular they are very weak for accretion rates higher than $\sim 10^{-6} M_{\odot} \text{ yr}^{-1}$.

The envelope mass at the ignition depends also on the core temperature. If the core temperature of the initial WD is lower

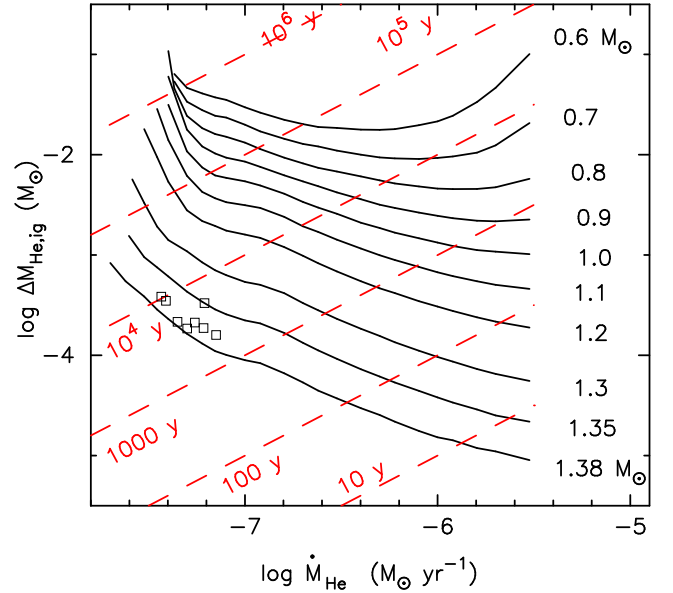


FIG. 7.— The helium ignition mass, $\Delta M_{\text{He,ig}}$, of helium-accreting WDs is plotted against the helium accretion rate, \dot{M}_{He} . The WD mass is attached to each curve. Straight dashed lines indicates the recurrence period. The open square indicates the ignition mass of each model in Table 2.

than that of the steady state model employed for our calculations, the envelope mass at the ignition would be larger.

The recurrence period, $\Delta M_{\text{He,ig}}/\dot{M}_{\text{He}}$, is also plotted in Figure 7 by dashed lines. The recurrence period corresponding to the ignition mass of our fitted models are listed in Table 2.

5.3. Mass Transfer from Helium Star Companion

We have estimated the mean accretion rate \dot{M}_{He} of the WD as in Table 2. The companion star feeds its mass to the WD via the Roche lobe overflow or by winds depending on whether it fills the Roche lobe or not. Here we examine if this accretion rate is comparable to the mass transfer rates of the Roche lobe overflow from a helium star companion. We followed stellar evolutions of helium stars from the main sequence assuming that the star always fills its effective Roche lobe of which radius is simply assumed to be $1.5 R_{\odot}$. The resultant mass loss rates are shown in Figure 8 for stars with initial masses of 1.2, 1.0 and $0.8 M_{\odot}$. These results are hardly affected even if we change the Roche lobe radius.

The mass loss rate decreases with the companion mass almost independently of the initial value. Except for the short initial and final stages, these rates are as large as $\dot{M}_{\text{He}} \sim 10^{-6} M_{\odot} \text{ yr}^{-1}$ and much larger than the mass accretion rate estimated from our fitted models in Table 2. Since almost all of the mass lost by the companion accretes onto the WD in the case of Roche lobe overflow, the accretion may result in very weak shell flashes for such high rates as $10^{-6} M_{\odot} \text{ yr}^{-1}$. A strong shell flash like V445 Pup is realized only when the final stages of mass-transfer in which the mass transfer rate quickly drops with time. This rare case may correspond to a final stage of binary evolution after the WD had grown up in mass to near the Chandrasekhar limit from a less massive one and the companion had lost a large amount of mass via Roche lobe overflow. Such information will be useful for modeling a new path of binary evolution scenario that will lead to a Type Ia supernova.

5.4. Comparison with Other Observation

³ <http://www.kusastro.kyoto-u.ac.jp/vsnet/Mail/alert5000/msg00493.html>

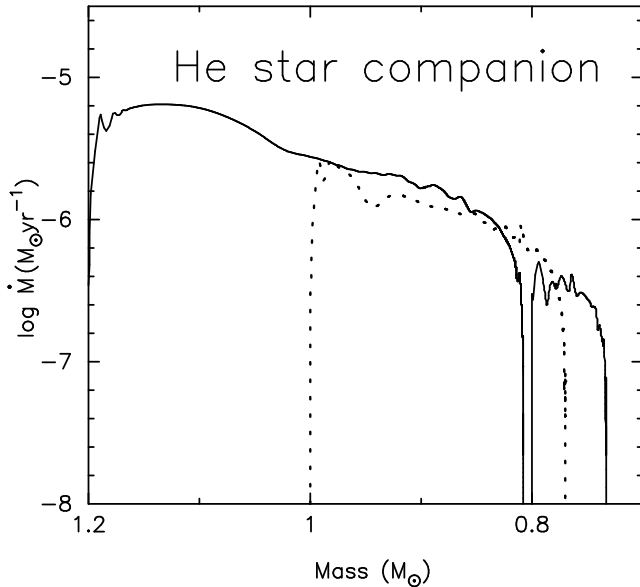


FIG. 8.— Mass loss rate of a helium star that fills its Roche lobe of the radius $1.5 R_{\odot}$. The initial stellar mass is 1.2, 1.0 (dotted line), and $0.8 M_{\odot}$. Time goes from left to right. See the text for more detail.

The mass of the dust shell can be estimated from infrared continuum flux with the assumption that the emission originated from warm dust. With infrared $10 \mu\text{m}$ spectrum, Lynch et al. (2004b) estimated the dust mass to be $2 \times 10^{-6} M_{\odot}$ for a distance of 3 kpc. This value would be increased if we adopt a larger distance instead of 3 kpc, but still consistent with our estimated ejecta mass $\Delta M_{\text{ej}} \sim (0.7 - 1.8) \times 10^{-4} M_{\odot}$ in Table 2, because the dust mass is a small part of the ejected mass.

Lynch et al. (2004a) reported the absence of He II or coronal lines on their near IR spectra and suggested that the ionizing source was not hot enough on 2004 January 14 and 16 (1146 days after the optical maximum). Lynch et al. (2005) also reported, from their near IR observation on 2005 November 16 that the object had faded and the thermal dust emission had virtually disappeared. They suggested that the dust had cooled significantly until that date (1818 days). This suggestion may constrain the WD mass of V445 Pup because Figure 4 shows the outburst lasts more than 1800 days for less massive WDs ($\lesssim 1.33 M_{\odot}$). If the WD had cooled down until the above date we may exclude less massive WD models ($\lesssim 1.33 M_{\odot}$) because these WDs evolve slowly and their hot surfaces emit high energy photons at least until 1800 days after the optical peak.

We have shown that the WD mass of V445 Pup is increasing with time. When the WD continues to grow up to the Chandrasekhar limit, central carbon ignition triggers a Type Ia supernova explosion if the WD consists of carbon and oxygen. We regard the star as a CO WD instead of an O-Ne-Mg WD because no indication of neon were observed in the nebula phase spectrum (Woudt & Steeghs 2005). Therefore, we consider that V445 Pup is a strong candidate of Type Ia supernova.

When a binary consisting of a massive WD and a helium star like V445 Pup becomes a Type Ia supernova, its spectrum may more or less show a sign of helium. The search for

such helium associated with a Type Ia supernova has been reported for a dozen Type Ia supernovae (Marion et al. 2001; Mattila et al. 2005), but all of them are negative detection. It may be difficult to find such a system because this type of Type Ia supernovae are very rare.

The binary seems to be still deeply obscured by the optically thick dust shell even several years after the outburst. This blackout period is much longer than that of the classical novae such as OS And (~ 20 days), V705 Cas (~ 100 days), and DQ Her (~ 100 days). As the ejected mass estimated in Table 2 is not much different from those of classical novae, the difference of the blackout period may be attributed to a large amount of dust in the extremely carbon-rich ejecta of a helium nova. Moreover, observed low ejection velocities of $\sim 500 \text{ km s}^{-1}$ (Iijima & Nakanishi 2007) is not much larger than the escape velocity of the binary with a relatively massive total mass [e.g., $1.35 M_{\odot} + (1 - 2) M_{\odot}$]. Both of these effects lengthen the dust blackout period. When the dust obscuration will be cleared in the future the period of blackout provides useful information on the dust shell.

6. CONCLUSIONS

Our main results are summarized as follows:

1. We have reproduced V and I_c light curves using free-free emission dominated light curves calculated on the basis of the optically thick wind theory.
2. From the light curve analysis we have estimated the WD mass to be as massive as $M_{\text{WD}} \gtrsim 1.35 M_{\odot}$.
3. Our light curve models are now consistent with a longer distance of $3.5 \lesssim d \lesssim 6.5$ kpc (Iijima & Nakanishi 2007) and 4.9 kpc (Woudt & Steeghs 2008).
4. We have estimated the ejecta mass as the mass lost by optically thick winds, i.e., $\Delta M_{\text{wind}} \sim 10^{-4} M_{\odot}$. This amounts to about a half of the accreted helium matter so that the accumulation efficiency reaches $\sim 50\%$.
5. The white dwarf is already very close to the Chandrasekhar mass, i.e., $M_{\text{WD}} \gtrsim 1.35 M_{\odot}$, and the WD mass had increased after the helium nova. Therefore, V445 Pup is a strong candidate of Type Ia supernova progenitors.
6. We emphasize importance of observations after the dense dust shell will disappear, especially observations of the color and magnitude, orbital period, and inclination angle of the orbit. These are important to specify companion nature.

M.K. and I.H. are grateful to people at the Astronomical Observatory of Padova and at the Department of Astronomy of the University of Padova, Italy, for their warm hospitality. Especially we thank Takashi Iijima for fruitful discussion on V445 Pup, which stimulated us to start this work. The authors thank Masaomi Tanaka for information on the helium detection in Type Ia supernovae. We also thank the anonymous referee for useful comments to improve the manuscript. Thanks are also due to the American Association of Variable Star Observers (AAVSO) for the photometric data of V445 Pup and Taichi Kato for introducing us the discussion in VSNET. This research has been supported in part by the Grants-in-Aid for Scientific Research (16540211, 20540227) from the Japan Society for the Promotion of Science.

REFERENCES

- Brown, R. L., & Mathews, W. G. 1970, *ApJ*, 160, 939
- Ferland, G. J. 1977, *ApJ*, 215, 873
- Gallagher, J. S., & Ney, E. P. 1976, *ApJ*, 204, L35
- Hachisu, I., & Kato, M. 2003, *ApJ*, 590, 445
- Hachisu, I., & Kato, M. 2006, *ApJS*, 167, 59
- Hachisu, I., & Kato, M. 2007, *ApJ*, 662, 552
- Hachisu, I., Kato, M., & Cassatella, A. 2007, *ApJ*, submitted
- Hachisu, I., Kato, M., Kato, T., & Matsumoto, K. 2000, *ApJ*, 528, L97
- Hachisu, I., Kato, M., Luna, G.J.M., *ApJ*, 2007, 659, L153
- Hachisu, I., Kato, M., & Nomoto, K. 1999a, *ApJ*, 522, 487
- Henden, A. A., Wagner, R. M., & Starrfield, S. G., 2001, *IAU Circ.*, 7730
- Iglesias, C. A., & Rogers, F. J. 1996, *ApJ*, 464, 943
- Iijima, T., & Nakanishi, H. 2008, *A&A*, in press
- Kamath, U. S., & Anupama, G. C. 2002, *Bull. Astr. Soc. India*, 30, 679
- Kato, M., & Hachisu, I. 1994, *ApJ*, 437, 802
- Kato, M., & Hachisu, I. 1999, *ApJ*, 513, L41
- Kato, M., & Hachisu, I. 2003, *ApJ*, 598, L107
- Kato, M. & Hachisu, I. 2004, *ApJ*, 613, L129
- Kato, M., Saio, H., & Hachisu, I. 1989, *ApJ*, 340, 509
- Kato, T., & Kanatsu, K., 2000, *IAU Circ.* 7552
- Kolotilov, E. A., & Liberman, A. A. 1976, *Soviet Astron. Lett.*, 2, 37
- Lynch, D. K., Rudy, R.J., Mazuk, .S, & Venturini, C.C. 2004a, *IAU Circ.*, No. 8278
- Lynch, D. K., Rudy, R.J., Mazuk, .S, & Venturini, C.C. 2004b, *AJ*, 128, 2962
- Lynch, D. K., Rudy, R. J., Venturini, C. C., Mazuk, S., Puetter, R.C., Perry, R. B., & Walp, B. 2005, *IAU Circ.* No. 8642
- Marion, G.H., Höflich, P., Vacca, W.D., & Wheeler, J.C. 2003, *ApJ*, 591, 316
- Mattila, S., Lundqvist, P., Sollerman, J., Kozma, C., Baron, E., Fransson, C., Leibundgut, B., & Nomoto, K. 2005, *A&A*, 443, 649
- McGowan, K. E., Charles, P. A., Blustin, A. J., Livio, M., O'Donoghue, D., & Heathcote, B. 2006, *MNRAS*, 364, 462
- Nomoto, K., Thielemann, F., & Yokoi, K. 1984, *ApJ*, 286, 644
- Paczynski, B. 1971, *Acta. Astron.*, 21, 1
- Saio, H. 1995, *MNRAS*, 277, 1393
- Schmidtke, P. C. & Cowley, A. P. 2006, *AJ*, 131, 600
- Shenavrin, V. I., & Moroz, V. I. 1976, *Soviet Astron. Lett.*, 2, 39
- Webbink, R.F., Livio, M., Truran, J.W., & Orio, M. 1987 *ApJ*, 314, 653
- Woudt, P.A., & Steeghs, D. 2005, in *ASP Conf. Ser., The Astrophysics of Cataclysmic Variables and Related Objects*, ed. J.M. Hameury & J.P. Laota (San Francisco: ASP), 330, 451
- Woudt, P.A., 2002, *IAU Circ.*, No.7955
- Woudt, P.A., & Steeghs, D., 2008, in *ASP Conf. Ser., Hydrogen-Deficient Stars*, Ed. K. Werner, & T. Rauch (San Francisco: ASP), in press